Vol. 38 (2007) ACTA PHYSICA POLONICA B No 4

NUCLEAR REACTIONS USED TO PROBE THE STRUCTURE OF NUCLEI FAR FROM STABILITY* **

J.A. Tostevin

Department of Physics, School of Electronics and Physical Sciences
University of Surrey, Guildford, Surrey GU2 7XH, UK

(Received January 2, 2007)

The study of nucleon pairing phenomena and of nucleon pair correlations, particularly in very neutron-rich or neutron-deficient exotic nuclei, is of considerable interest. This paper begins to address the capabilities of fast two-nucleon knockout reactions to make a positive contribution to such studies. Specifically, we address the sensitivity of two-nucleon knockout partial reaction cross-sections (and the associated momentum distributions of the reaction residues), measured by the combination of particle and coincident gamma-ray detection, to the details of (a) nuclear structure models (here the large-basis shell model), (b) the removed nucleons' wave function configurations, and their ability to investigate nucleon pair-correlations in exotic nuclei. We do this by combining recent theoretical and experimental developments.

PACS numbers: 21.10.Jx, 24.10.–i, 25.60.Gc, 27.30.+t

1. Introduction

Studies of very exotic nuclei are revealing a complex evolution of nucleon single-particle states with increasing neutron and proton asymmetry. Final-state-exclusive, fast single nucleon knockout reactions at fragmentation energies, measured using a combination of particle and gamma-ray spectroscopy, continue to play a key part in untangling this evolution of states, see *e.g.* [1, 2]. The large intrinsic cross-sections and high experimental efficiency and selectivity of these reactions allow a mapping of the energies, angular momenta, ordering and spectroscopic strengths of the single-particle

* Presented at the Zakopane Conference on Nuclear Physics, September 4–10, 2006, Zakopane, Poland.
** Supported by the UK Engineering and Physical Sciences Research Council (EPSRC) under Grant No. EP/D003628.

configurations at both the tightly-bound (deficient nucleon species) and the weakly-bound (excess nucleon species) Fermi surfaces. Good examples can be found in Refs. [3, 4] and references therein. Furthermore, the reactions have been shown to provide quantitative spectroscopic information [5], of single nucleon spectroscopic factors, a long-standing ambition of direct reaction methodologies. Though necessarily more complicated, and having smaller intrinsic cross-sections, measurements of fast (direct) two-nucleon knockout reactions may be able to provide unique additional information, particularly on the role of nucleon correlations and pairing in such rare, asymmetric systems.

The study of nucleon pairing phenomena [6] and of nucleon pair correlations, particularly in very neutron rich or neutron deficient exotic nuclei, is of considerable interest. Among the reactions that result in the removal of two like nucleons from a nucleus are (a) light-ion induced two-nucleon transfer reactions, such as the (p,t) reaction [7], (b) the $(e,e'pp)$, electron induced two-proton knockout reaction, [8] and references therein, and more recently (c) two-proton decay of nuclei near the proton dripline, *e.g.* [9] and references therein. All of these will manifest sensitivity to the pairing interaction between like nucleons and to *(i)* the associated transition strengths and *(ii)* the coherence of the two-nucleon configurations. However, in the latter two reactions, theoretical analyses are complicated considerably by the presence of strong final-state interactions of the two emergent nucleons in the few-body final states. Two-nucleon transfer and electron-induced two proton knockout reactions are not yet available for spectroscopy studies using very rare secondary beams.

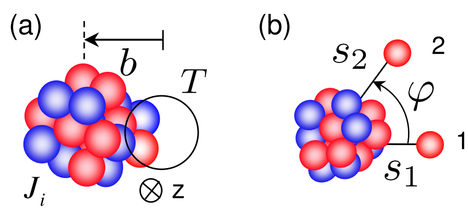

Fig. 1. Representation of the cylindrical volume probed by the target (T) in the direct two-nucleon knockout mechanism (a). The two-removed-nucleon position coordinates, both shown in the (impact parameter) plane normal to the beam direction, the z-direction (b).

Very recently, first measurements have been made of fast two-nucleon knockout reactions from exotic secondary fragmentation beams by a light nuclear target [10–13]. The high energy (and speed) of such collisions, of the order of 100 MeV/nucleon, allow the use of accurate approximations (sudden/adiabatic, eikonal/Glauber and forward scattering) to the treatment of the many-body dynamics, and thus of simplified reaction dynamical approaches. Further details can be found in Refs. [14,15]. Structurally, such reactions probe the same two-nucleon transition densities, *e.g.* [14,16], that enter the other reactions referred to above, such as (p,t) and/or $(e,e'pp)$, but now (a) in distinct regions of the nuclear chart, and (b) with somewhat different spin and spatial sensitivity to the two removed nucleons' wave functions, see Fig. 1(a). The reactions we consider here involve, principally, the direct removal of pairs of well-bound like nucleons of the deficient species.

2. Knockout of nucleons of the excess species

Two neutron removal from ($A+2$ body) neutron rich systems is also of considerable interest, to look for novel neutron pair correlations in the neutron halo and skin regions.

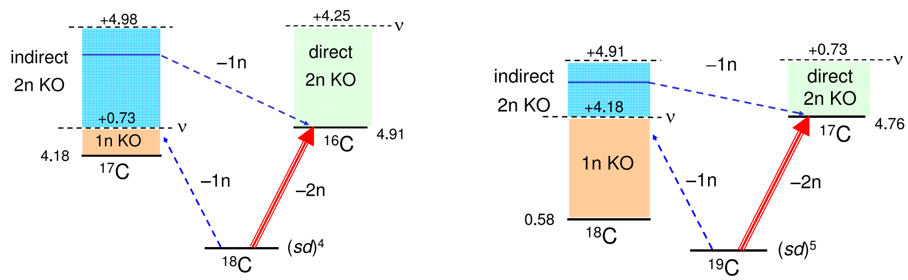

Fig. 2. Schematic of the nucleon threshold energies relevant to one- and two-neutron removal reactions from ^{18}C (left panel) and from ^{19}C (right panel). In both cases, there will be strength for excitations to states, of only modest excitation energy, but above the neutron evaporation thresholds of the intermediate ($A+1$ body) fragments. These will be populated by single-neutron removal (dashed arrows) and will lead to indirect feeding of the A body residues (dashed paths) in competition with direct removal contributions (indicated by the solid arrows).

However, as is depicted in Fig. 2, for ^{18}C (left panel) and ^{19}C (right panel) projectiles, the low neutron separation thresholds of the ($A+1$ body) intermediate fragments, that will be populated in one-neutron removal events, means that two neutron removal will arise from both direct and two-step (single nucleon knockout followed by evaporation) events. The reactions are thus significantly more difficult to interpret, requiring knowledge of the one-nucleon excitation strength into the continuum. However, they also require, as an essential component, an accurate calculation of the direct cross-sections (represented by the solid arrows). This paper concerns validating these direct contributions using removal of nucleons of the deficient species where the reactions are then entirely direct, see discussions in Refs. [10,14].

It is interesting to note, however, that along the carbon isotopic chain, two members of which are represented in Fig. 2, there is significant odd–even staggering of the physical neutron separation energies — and hence in the anticipated single particle strengths that will lead to unbound intermediate states. These should lead also to a staggering in the indirect-path yields for projectiles along the isotopic chain and should allow a first assessment of the magnitudes of the competing direct and indirect two-neutron removal contributions. This is work in progress.

3. Knockout of nucleons of the deficient species

The example reactions used here are *(i)* two-proton removal from neutron rich ^{28}Mg at 83.2 MeV/nucleon [10], and *(ii)* two-neutron knockout from neutron deficient ^{34}Ar, ^{30}S, and ^{26}Si, at ≈ 100 MeV/nucleon [11], all performed at the NSCL on a ^{9}Be secondary target. The structure models used are the large basis shell model and also, when neglecting explicit pair correlations, the independent particle shell model. The nuclear structures enter through the overlap functions for two nucleons in the projectile ground state, relative to a specified (A body) residue final state JM, and are, in general, the sum over several contributing configurations [15]

$$\langle \Phi_{JM} | \Psi_{J_i M_i}(1,2)\rangle = \sum_{I\mu\alpha} C_\alpha^{J_i J I} (I\mu J M_f | J_i M_i) [\overline{\phi_{j_1}(1) \otimes \phi_{j_2}(2)}]_{I\mu} \,. \tag{1}$$

Here $\alpha \equiv \{n_1\ell_1 j_1, n_2\ell_2 j_2\}$ denotes each pair of orbitals and the $C_\alpha^{J_i J I}$ are the two-nucleon amplitudes that carry the structure calculation details. The knockout reaction's sensitivity to details of these microscopic two-nucleon wave functions is therefore accessible by interrogating the wave function in the reaction-sampled volume, as was shown in Fig. 1(a). In a transition from an even–even spin-0 projectile the microscopic two-nucleon transition density is then

$$F_J^M(1,2) = \sum_\alpha (-1)^{J+M} C_\alpha^{0JJ} / \hat{J}\, [\overline{\phi_{j_1} \otimes \phi_{j_2}}]_{J-M} \,. \tag{2}$$

We consider the (final state) J-dependence of *(i)* the position probabilities, $P_J(\vec{s}_1, \vec{s}_2)$, that the two (point) nucleons (1,2) will be found with values of s_1 and s_2 (near the projectile surface) with an angular separation φ, see Fig. 1(b), and *(ii)* the associated differential probabilities $P_J(\vec{s}_1, \vec{s}_2, K)$ that the total z-component of momentum of the nucleons, and hence that of the residue, is K.

The correlated, beam-direction-integrated position probability densities are, in more detail

$$P_J(\vec{s}_1,\vec{s}_2) \propto \sum_M \int dz_1 \int dz_2 \left\langle F_J^M(1,2) | F_J^M(1,2) \right\rangle_{\rm sp} , \tag{3}$$

where $\langle \ldots \rangle_{\rm sp}$ denotes the integration over all spin variables. Using the notation of Ref. [15], then the position probabilities are

$$P_J(\vec{s}_1,\vec{s}_2) \propto \sum_{\alpha\alpha'} D_\alpha D_{\alpha'} C_\alpha^{0JJ} C_{\alpha'}^{0JJ} \hat{j}_1 \hat{j}_2 \sum_{KQ} (-1)^Q \{\mathrm{dir} - \mathrm{exch}\}/\hat{K}^2 , \tag{4}$$

where the direct and exchange contributions are

$$\begin{aligned}
\mathrm{dir} \;&\equiv\; (-)^{J-j_1-j_2'}\, W(j_1 j_1' j_2 j_2'; KJ)\, \left\{ [j_1'\ell_1'|\mathcal{O}_{K-Q}(\vec{s}_1)|j_1\ell_1] \right. \\
&\times\; \left. [j_2'\ell_2'|\mathcal{O}_{KQ}(\vec{s}_2)|j_2\ell_2] + [j_1'\ell_1'|\mathcal{O}_{K-Q}(\vec{s}_2)|j_1\ell_1]\, [j_2'\ell_2'|\mathcal{O}_{KQ}(\vec{s}_1)|j_2\ell_2] \right\} , \\
\mathrm{exch} \;&\equiv\; (-)^{j_2'-j_1}\, W(j_1 j_2' j_2 j_1'; KJ)\, \left\{ [j_2'\ell_2'|\mathcal{O}_{K-Q}(\vec{s}_1)|j_1\ell_1] \right. \\
&\times\; \left. [j_1'\ell_1'|\mathcal{O}_{KQ}(\vec{s}_2)|j_2\ell_2] + [j_2'\ell_2'|\mathcal{O}_{K-Q}(\vec{s}_2)|j_1\ell_1]\, [j_1'\ell_1'|\mathcal{O}_{KQ}(\vec{s}_1)|j_2\ell_2] \right\} ,
\end{aligned}$$

and we have written the spin- and z-integrated single-particle products as

$$\int dz\ (\phi_{j'}^{m'}|\phi_j^m)_{\rm sp} = \sum_{KQ} (j'm'KQ|jm)\, [j'\ell'|\mathcal{O}_{KQ}(\vec{s})|j\ell] . \tag{5}$$

In this explicit form, the correlations arising from (a) the $K \neq 0$ terms, and (b) the coherence of the different active α contributions, are both evident. If the two bound nucleons are completely uncorrelated and uncoupled, being simply bound to the same core, then the analogous probability is of course

$$P(s_1,s_2) \propto \sum_{mm'} \int dz_1\ (\phi_j^m|\phi_j^m)_{\rm sp} \int dz_2\ (\phi_j^{m'}|\phi_j^{m'})_{\rm sp} , \tag{6}$$

and which removes both the interesting J and the φ dependence.

4. Sensitivity to pair and other correlations

The importance of these correlations on the probabilities in the reaction-sampled volume, as a function of the coordinates of Fig. 1(b), are demonstrated in Fig. 3 for the case of two-proton removal from neutron-rich ^{28}Mg. This is, dominantly, a $\pi[d_{5/2}]^2$ proton pair removal. The left panel shows the φ-dependence of the $P_J(s,s,\varphi)$ at the nuclear surface with $s = 2.5$ fm, assuming a pure $\pi[d_{5/2}]^2$ proton removal — *i.e.* a single α=$\pi[d_{5/2}]^2$ configuration.

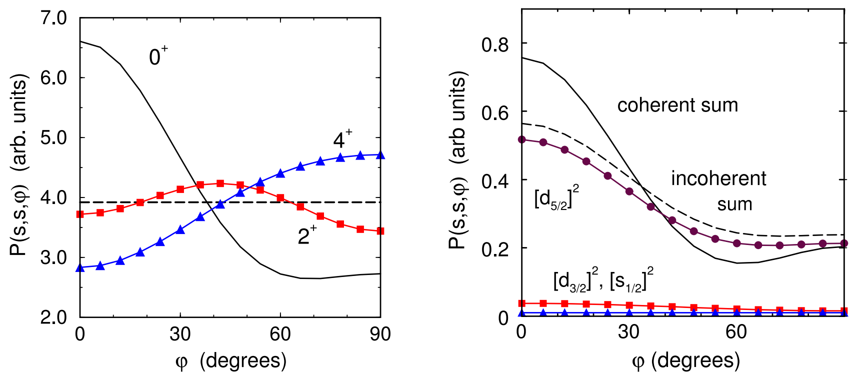

Fig. 3. Left: The φ-dependence of the two nucleon position probabilities $P_J(s,s,\varphi)$, $s = 2.5$ fm, for $[d_{5/2}]^2$ proton removal from ^{28}Mg. The curves show the changes from the completely uncorrelated limit. Right: The analogous φ-dependence of the 0^+ state two-proton position probability $P_0(s,s,\varphi)$ from the USD shell model wave function. The (correct) fully-coherent and (for comparison) the incoherent density are shown.

The curves show the changes from the completely uncorrelated limit, represented by the (constant) dashed line, and show the enhanced probability at small two-proton separations in the 0^+ state transition density.

The further enhancement of the 0^+ state probability due to the coherence of the multiple α configurations (of a full sd-shell shell model calculation) is shown in the right panel. The importance of the coherence of the dominant $\pi[d_{5/2}]^2$ and the (in this case) smaller contributions from the other α, in Eq. (4), are shown by comparing both the coherent and the incoherent combinations shown there. It is already clear therefore that the relative magnitudes of the final state cross-sections will sample both the pairing correlations and small components in the many-body (shell model) wave functions. Their importance will depend on the particular reaction, of the proximity to shell closures and gaps, and the degree of configuration mixing. It is encouraging, however, that even for the $\pi[d_{5/2}]^2$ dominant case above, the configuration mixed contributions are enhanced as a result of their coherence and are seen to be probed and manifest in the two-nucleon position probability density and the cross-sections [16].

5. Results for partial cross-sections

To further elucidate this expected enhancement of the 0^+ state probabilities, and cross-sections, and the associated suppression of the higher J final state yields compared to uncorrelated estimates, we consider the recent measurements for the two-neutron knockouts from neutron deficient ^{34}Ar, ^{30}S, and ^{26}Si, all carried out at ≈ 100 MeV/nucleon [11].

In Fig. 4 we show the measured and calculated ground state branching ratios in these cases, defined as the ratio of the ground state cross-section to the inclusive cross-section to all bound final states [11,15]. The methodology used for the cross-section calculations and a discussion of the measured and calculated absolute cross-sections can be found in Refs. [14,15]. The experimental values (filled diamonds) and those calculated using the full many-body shell model wave functions (filled squares) are in excellent agreement. The values calculated assuming two uncorrelated neutrons (filled circles) considerably underestimate the 0^+ ground state yields, consistent with the densities shown in Fig. 3 and the discussion above.

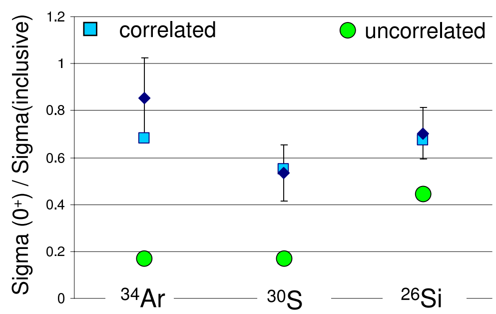

Fig. 4. Ground state branching ratios in two-neutron removal from ^{26}Si, ^{30}S and ^{34}Ar from experiment (filled diamonds), and calculated assuming two uncorrelated (circles) and many-body shell model wave functions (squares) for the two neutrons. See also Refs. [11,15].

6. Results for residue momentum distributions

A new feature of the present work, and a significant test and indicator of the directness of the reaction mechanism, is to now consider the momentum distributions of the (A body) reaction residues and their final state dependence.

To date, only inclusive residue momentum distributions have been measured in the case of two-nucleon knockout reactions [10,12]. In one nucleon removal the partial momentum distributions are a powerful spectroscopic diagnostic, with widths sensitive to the angular momentum of the removed nucleons. In two-nucleon knockout, in the limit that the two nucleons are completely uncorrelated, the predicted momentum distributions are obtained by convoluting the distributions for removal of each nucleon individually [10]. These uncorrelated distributions, when convoluted with the incident beam momentum profiles, were consistent with the broad distributions observed in Refs. [10,12] within the limited statistics of the experiments. A first estimate of the sensitivity of two-nucleon knockout partial momentum distributions to different residue final states can be obtained by looking at the momentum content of the correlated two-nucleon wave functions within the volume sampled by the target nucleus, Fig. 1(a).

We have calculated the probability $P_J(\vec{s}_1, \vec{s}_2, K)$ that, with the two nucleons at positions $\vec{s}_1$ and $\vec{s}_2$ in the plane perpendicular to the beam direction, Fig. 1(b), the residue has a z-component of momentum K, referred to the rest frame of the projectile. Explicitly therefore

$$P_J(\vec{s}_1, \vec{s}_2, K) = \sum_M \Big\langle \int dk_1 \int dk_2 \; \delta(K + k_1 + k_2) \times \left| \int dz_1 \int dz_2 \, e^{ik_1 z_1} e^{ik_2 z_2} F_J^M \right|^2 \Big\rangle_{\rm sp} . \quad (7)$$

The resulting residue distributions, for $s_1 = s_2 = 2.5$ fm and $\varphi = 10$ degrees, are shown in Fig. 5 for ^{28}Mg$\to$^{26}Ne(J^π) at 83.2 MeV on a ^{9}Be target. They display a very strong transition-dependence and that measured partial momentum distributions would have high spectroscopic value.

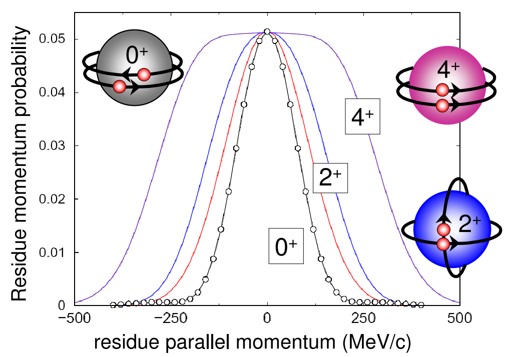

Fig. 5. Calculated residue momentum probabilities $P_J(s, s, \varphi, K)$ (with common normalisation at $K = 0$) for $s = 2.5$ fm and $\varphi = 10$ degrees. The results are for two-proton removal populating the 0^+, 2^+_1, 4^+ and 2^+_2 ^{26}Ne final states at 82.3 MeV per nucleon.

The widest components of the residue distributions are expected to arise from components in the wave function with nucleon velocities parallel to, or antiparallel to the beam direction. As is shown schematically, and because the ^{28}Mg$\to$ ^{26}Ne(J^π) reaction is predominantly $\pi[d_{5/2}]^2$ proton removal, one would expect the 2^+ and 4^+ final state residue distributions to be approximately once and twice the width, respectively, of that for a single $[d_{5/2}]$ proton removal. This is essentially what is observed. The narrow distribution calculated for the 0^+ transition results from the like-nucleon pairing. Measurements are now needed to test these theoretical predictions.

7. Summary remarks

In this paper we address the capabilities of fast two-nucleon knockout reactions to make a positive contribution to pairing studies. Specifically, we have looked at the sensitivity of the knockout partial reaction cross-sections to details of nuclear structure models and the removed nucleons' configurations. We have shown that the relative magnitudes of the final state cross-sections can probe both pairing correlations and small components in the many body (shell model) wave functions. A new feature of the present paper concerns the expected momentum distributions of the heavy (A body) reaction residues and their final state (J) dependence. We have shown that this observable may provide the clearest indication of both (a) the directness of the reaction mechanism, reinforcing our knowledge of the reaction dynamics, and (b) the J-value of the transition, allowing more detailed two-particle spectroscopy. This additional handle on the directness, or otherwise, of the reaction mechanism could be invaluable in untangling and quantifying contributions from direct and indirect mechanisms, as were discussed in Section 2 in relation to studies of two neutron removal from neutron rich systems. However, exclusive momentum distribution measurements in selected direct-reaction-dominated cases are first needed to confirm these new theoretical model predictions.

REFERENCES

[1] J.R. Terry *et al. Phys. Lett.* **B640**, 86 (2006).
[2] S.D. Pain *et al.*, *Phys. Rev. Lett.* **96**, 032502 (2006).
[3] P.G. Hansen, J.A. Tostevin, *Annu. Rev. Nucl. Part. Sci.* **53**, 219 (2003).
[4] A. Gade *et al.*, *Phys. Rev. Lett.* **93**, 042501 (2004).
[5] B.A. Brown, P.G. Hansen, B.M. Sherrill, J.A. Tostevin, *Phys. Rev.* **C65**, 061601 (2002).
[6] D.M. Brink, R.A. Broglia, *Nuclear Superfluidity: Pairing in Finite Systems*, Cambridge University Press, 2005.
[7] M.H. Macfarlane, J.P. Schiffer, in *Nuclear Spectroscopy and Reactions, Part B*, ed. J. Cerny, Academic Press, New York 1974, p. 169.
[8] C.J.G. Onderwater *et al.*, *Phys. Rev. Lett.* **81**, 2213 (1998).
[9] B.A. Brown, F.C. Barker, *Phys. Rev.* **C67**, 041304 (2003).
[10] D. Bazin *et al.*, *Phys. Rev. Lett.* **91**, 012501 (2003).
[11] K. Yoneda *et al.*, *Phys. Rev.* **C74** 021303 (2006).
[12] A. Gade *et al.*, *Phys. Rev.* **C74** 021302 (2006).
[13] J. Fridmann *et al.*, *Nature* **435**, 922 (2005); *Phys. Rev.* **C74**, 034313 (2006).
[14] J.A. Tostevin, G. Podolyák, B.A. Brown, P.G. Hansen, *Phys. Rev.* **C70**, 064602 (2004).
[15] J.A. Tostevin, B.A. Brown, *Phys. Rev.* **C74**, 064604 (2006).
[16] J.A. Tostevin, *J. Phys. Conf. Series* **49**, 21 (2006).